Molecular and Cellular Pathobiology

Strain-Specific Susceptibility for Pulmonary Metastasis of Sarcoma 180 Cells in Inbred Mice

Haris G. Vikis[1,5], Erin N. Jackson[3,4], Alexander S. Krupnick[1,5], Andrew Franklin[1], Andrew E. Gelman[1], Qiong Chen[1], David Piwnica-Worms[2,3,4,5], and Ming You[1,5]

Abstract

Most cancer deaths are a result of metastasis. To extend our understanding of the factors that influence the process, we aimed to develop a mouse model of pulmonary metastasis that can be assayed in multiple inbred mouse strains for further use in identification of host genetic variants that influence metastasis. We used i.v. injection of Sarcoma 180 (S180) cells, which can be tracked and quantified by bioluminescence imaging. We observed growth of S180 cells solely in the lung and observed a wide range of pulmonary metastasis among inbred mouse strains. Interestingly, we noted that the BTBRT+tf/J strain exhibited complete clearance and provide evidence that the mechanism of resistance may involve immune factors, as strains subjected to whole-body irradiation are significantly more susceptible to tumor growth. One possible mechanism of resistance to pulmonary metastasis in BTBRT+tf/J mice may require T-cell function. Our experiments present a new mouse model for further characterization of the genetics and mechanisms of pulmonary metastasis. *Cancer Res; 70(12); 4859–67. ©2010 AACR.*

Introduction

Metastasis is a multistep process that begins when a primary tumor acquires mutations and becomes invasive, and cells eventually enter into the blood or lymph (1). After transportation and avoidance of anoikis, cells may rest in an organ through adherence, extravasation, proliferation, and establishment within the microenvironment (2). Most tumor cells die from various stresses after they leave the primary tumor and only a low percentage of micrometastases progress into macrometastases after engraftment. The tissue microenvironment of the target organ, including stromal cells, stromal-associated cells (endothelium and macrophages), transient inflammatory cells, and parenchymal cells, in addition to tropic and angiogenic factors, influences metastatic growth (3). Metastases arise most commonly in the lung, liver, brain, and bone. Interestingly, the lung is the most common site for systemic sarcoma metastases because of the substantial vasculature that feeds into this organ, in addition to particular tropic factors (4). Other cancers that often metastasize to the lung include breast, colon, prostate, bladder, and various neuroblastomas (5).

Previous studies have focused on identifying somatic genetic events in tumor cells, as these cells acquire metastatic properties at the site of the primary tumor. These studies have mainly focused on elucidating a role of various adhesion receptors, proteases, and angiogenic factors (6, 7). However, limited knowledge exists on inherited susceptibility to metastasis and the underlying host genetic variants that influence the process. Most strategies aim to treat cancers only once a gross lesion has developed, and have, for the vast majority of cancers, not led to significant decreases in mortality. Hence, treatment and prevention strategies aimed to reduce the risk or delay the development or recurrence of cancer are one rational approach that can be aided through identification of host susceptibility factors.

Mouse models of metastasis may thus be useful; however, few exist to model the process (8). The few metastasis models that have been used, such as those for breast and prostate cancer, primarily rely on viral oncogenes (9, 10). Tumors induced by transgenes or carcinogens are not practical in studies of metastasis because they typically are less aggressive than human tumors, with weaker stromal reaction and very few metastases. One common lung metastasis model, using Lewis lung carcinoma cells, involves injecting cells s.c. into nude mice or syngeneic C57BL/6 mice (8). After allowing a tumor to grow to a particular size, it is excised, which can initiate pulmonary metastases. However, this model is only amenable to use with syngeneic cell lines and does not permit phenotyping in multiple inbred strains for further identification of genetic susceptibility variants in quantitative trait mapping using linkage and genome-wide association analysis.

The Sarcoma 180 (S180) mouse cell line is derived from a sarcoma carried in Swiss Webster mice and has been

Authors' Affiliations: [1]Department of Surgery, [2]Developmental Biology, [3]Molecular Imaging Center, [4]Mallinckrodt Institute of Radiology, and [5]Alvin J. Siteman Cancer Center, Washington University School of Medicine, St. Louis, Missouri

Corresponding Author: Ming You, Department of Surgery and the Alvin J. Siteman Cancer Center, Washington University School of Medicine, Campus Box 8109, 660 South Euclid Avenue, St. Louis, MO 63110. Phone: 314-362-9294; Fax: 314-362-9366; E-mail: youm@wudosis.wustl.edu.

American Association for **Cancer Research**

described to grow in multiple inbred mouse strains due to β_2-microglobulin deficiency, MHC class I destabilization, and lack of recognition by host CTLs (11). I.p. injection of these cells results in strain-dependent killing due to accumulation of ascites fluid (11, 12). Recent studies have identified a spontaneous mutant of the BALB/c mouse, termed the spontaneous resistance/complete regression (SR/CR) mouse, which exhibited resistance to S180 cell challenge. These studies suggested the existence of a resistance trait that is autosomal dominant and from a single locus (13–15).

Here, we describe an inbred mouse model of experimental pulmonary metastasis, which involves tracking of bioluminescent S180 cells that have been introduced i.v. into inbred strains of mice. These cells migrate to the lung and grow at varying rates in inbred strains. We have found that the BTBRT strain shows complete resistance in this experimental metastasis model. Our studies further implicate a role of the immune system and T cells in response to S180 cell challenge and suggest the framework for a model for the determination of the genetic susceptibility of pulmonary metastasis.

Materials and Methods

Cell culture and transfection

S180 cells were purchased from the American Type Culture Collection and grown in DMEM in the presence of 10% fetal bovine serum. To create a constitutively expressing luciferase cell line, S180 cells were transfected with linearized pUB6-*Fluc*-mNLS-*SR39TK*-IRES-*MGFP* and selected for 2 weeks in the presence of 5 µg/mL blasticidin (16). Individual clones were selected, plated in equal numbers, and imaged for bioluminescence after incubation for 10 minutes with 150 µg/mL D-luciferin in modified Earle's balanced salt solution at 37°C. Cells were imaged with a charge-coupled device camera–based bioluminescence imaging system (IVIS 100, Caliper; exposure time 1–60 s, binning 8, field of view 15 cm, f/stop 1, open filter). Signal on images was displayed as photons/s/cm^2/sr (17, 18). Corresponding grayscale photographs and color luciferase images were superimposed and analyzed with Living Image (Xenogen) and Igor (Wavemetrics) image analysis software. Analyzed data were expressed as normalized photon flux (photons/s). The clone with the highest photon flux was selected, termed S180-Fluc, and used for further studies.

Injection and imaging studies

Inbred mouse strains were purchased from The Jackson Laboratory and for the multistrain assay included A/J (*n* = 10), DBA/2J (*n* = 9), FVB/NJ (*n* = 5), C57BL/6J (*n* = 9), AKR/J (*n* = 5), NZW/LacJ (*n* = 5), C57BR/cdJ (*n* = 5), SM/J (*n* = 5), and BTBRT+tf/J (*n* = 4). Female mice were delivered at 6 weeks of age and injected at 8 weeks. For injections and bioluminescence imaging in inbred strains, S180-Fluc cells were grown, trypsinized, and harvested in HBSS (+5% fetal bovine serum). Cells were passed through a cell strainer to remove clumps and counted by a hemacytometer. Cells were diluted to 3.5×10^6 cells/mL and injected (0.2 mL, 7×10^5 cells) into the lateral tail vein using a 0.3-mL syringe fitted

with a 29.5-gauge needle. Chest hair was depilated with Magic Gold shaving powder to control for coat color effects on signal output. For bioluminescence imaging of living animals, mice were injected i.p. with 150 µg/g D-luciferin (Biosynth) in PBS, anesthetized with 2.5% isoflurane, and imaged as described above. Regions of interest were defined manually over the thorax using Living Image and Igor Pro software. Data were analyzed by background subtraction and plotted as log(photons/s). S180-Fluc cells were also tested for viability by trypan blue dye exclusion assay and were determined to be 100% viable from the time of harvest to after the injection of the last mouse in the group.

Histology

Lungs were removed from A/J and BTBRT mice at 15 days after S180-Fluc injection (7×10^5 cells), inflated (25 cm of gravity) with Tellyesniczky solution (70% ethanol, 2% formaldehyde, and 5% acetic acid), and allowed to fix overnight. Solution was exchanged to 70% ethanol and lungs were embedded in paraffin stained with H&E. Lung sections were also stained using anti–proliferating cell nuclear antigen (PCNA; rabbit) and control anti-hemagglutinin probe (rabbit) antibodies. All histology preparation was done at the Digestive Disease Research Core Center at Washington University School of Medicine.

Cesium-137 γ-irradiation

A/J (*n* = 5) and BTBRT (*n* = 5) mice (with Bactrim antibiotic in drinking water) were treated with supralethal irradiation (18 Gy) from a cesium source and, along with nonirradiated control mice (*n* = 5 per strain), received 7×10^5 S180-Luc cells via tail vein injection within 4 hours of irradiation. Bioluminescent imaging of the thorax was done at days 1, 2, 3, and 7.

Flow cytometry

A/J and BTBRT mice were injected with S180-Fluc cells, and 1 and 7 days later, lungs were removed, digested, and prepared for flow cytometry as previously described (19). All antibodies used were purchased from BD Pharmingen or eBioscience and conjugated with fluorescein isothiocyanate (FITC), phycoerythrin, peridinin chlorophyll protein (PerCP), allophycocyanin (APC), or APC-eFluor® 780 (ebioscience). Sorting was done on a MoFlow (Dako-Cytomation) sorter at the High-Speed Cell Sorter Core of the Siteman Cancer Center at Washington University School of Medicine.

T-cell depletion

BTBRT mice were injected i.p. with anti-CD4 (GK1.5, BioXcell) and anti-CD8 (53.6.72, BioXcell) antibodies or normal rat IgG (BioXcell; 250 µg/mouse) every 2 days (five mice per group), beginning 4 days before S180-Fluc (7×10^5) tail vein injection. Antibody injection was continued and bioluminescent imaging of the lung was done at days 1 and 7.

Results

The aim of this study was to develop a mouse model of pulmonary metastasis that can be applied to and quantified

in multiple inbred strains of mice. The utility of developing such a model is that identification of strain-dependent phenotypes in inbred strains can be used for gene discovery using linkage studies and whole genome association analysis. However, few cell lines that are introduced i.v. will survive the host immune system in multiple inbred strains. S180 cells have previously been shown to grow in the peritoneum of multiple inbred strains; hence, we created an S180 cell line (S180-Fluc) constitutively expressing Firefly luciferase. Previously published studies on S180 cell–induced mouse death by i.p. delivery showed that A/J strain mice survived 2 to 3 weeks after injection (11). Guided by these observations, we introduced S180-Fluc cells (2×10^5 and 7×10^5) via the lateral tail vein into 8-week-old female A/J mice. We postulated that the S180-Fluc cells would enter the venous system, travel through the heart, and form emboli or migrate across the vascular endothelium to establish tumors in the lung. Whole-body bioluminescence imaging was done at 1, 7, and 15 days after S180-Fluc injection and bioluminescent signal was consistently and predominantly observed over the thorax (Fig. 1A). Thoracotomy and dissection of the thorax followed by imaging directly showed a bioluminescent signal in the lungs, and further removal of the lungs revealed gross enlargement of all lobes compared with a control injected A/J mouse at 15 days after injection (Fig. 1B). The signal in the area over the lungs increased

~1,000-fold from day 1 to day 15 (Fig. 1C). Death of A/J strain mice occurred between days 15 and 21 solely due to tumor growth in the lung, as determined by whole-body necroscopy in which the signal magnitude was generally in the 10^9 to 10^{10} photons/s range (data not shown).

Determination of a differential strain response to S180-Fluc tumor cell challenge would suggest host genetic control of the phenotype. We tested nine strains (A/J, FVB/NJ, C57BL/6J, NZW/LacJ, SM/J, DBA/2J, C57BR/cdJ, AKR/J, and BTBRT+tf/J) for their response to pulmonary tumor phenotypes. Tumor bioluminescence data were quantified in the region of interest of the lungs on days 1 and 7 after injection with 7×10^5 S180-Luc cells. Bioluminescent signal in the lungs of most inbred strains at day 7 ranged from 10^6 to 10^8 photons/s (Fig. 2A). However, no signal above background was observed in the lungs of BTBRT (BTBRT+tf/J) mice at day 7 (Fig. 2B and C). Interestingly, the BTBRT strain was the only strain tested that did not die. These mice remained healthy even several months later, suggesting complete clearance of S180 cells. We also tested to see whether the BTBRT strain was resistant to S180 cells by i.p. injection of 7×10^5 S180-Luc cells. Contrary to what was observed by i.v. injection through the tail vein, both A/J and BTBRT strains were susceptible to S180 cell–induced death by i.p. injection, suggesting that the pulmonary environment prevented the growth and/or facilitated the clearance of S180 tumor cells (Fig. 2D).

Figure 1. Phenotyping of pulmonary metastasis of bioluminescent S180-Fluc cells in A/J strain. A, A/J mice (n = 5) were tail vein injected with either 2×10^5 (low) or 7×10^5 (high) S180-Fluc cells. Bioluminescence signal [mean photon flux (photons/s)] was determined in the area over the lungs on days 1, 7, and 15 (shown are two representative mice at the 7×10^5 dose). B, thoracotomy and dissection of the thorax was done, followed by imaging directly in an A/J mouse 15 d after S180-Fluc injection (left). Lungs from an A/J mouse injected with media control or with 7×10^5 S180-Fluc cells were removed after 15 d, fixed in Telly's solution, and photographed (right). C, lung bioluminescence was quantified for 2×10^5 and 7×10^5 S180-Fluc cell doses on days 1, 7, and 15. Bars, SD.
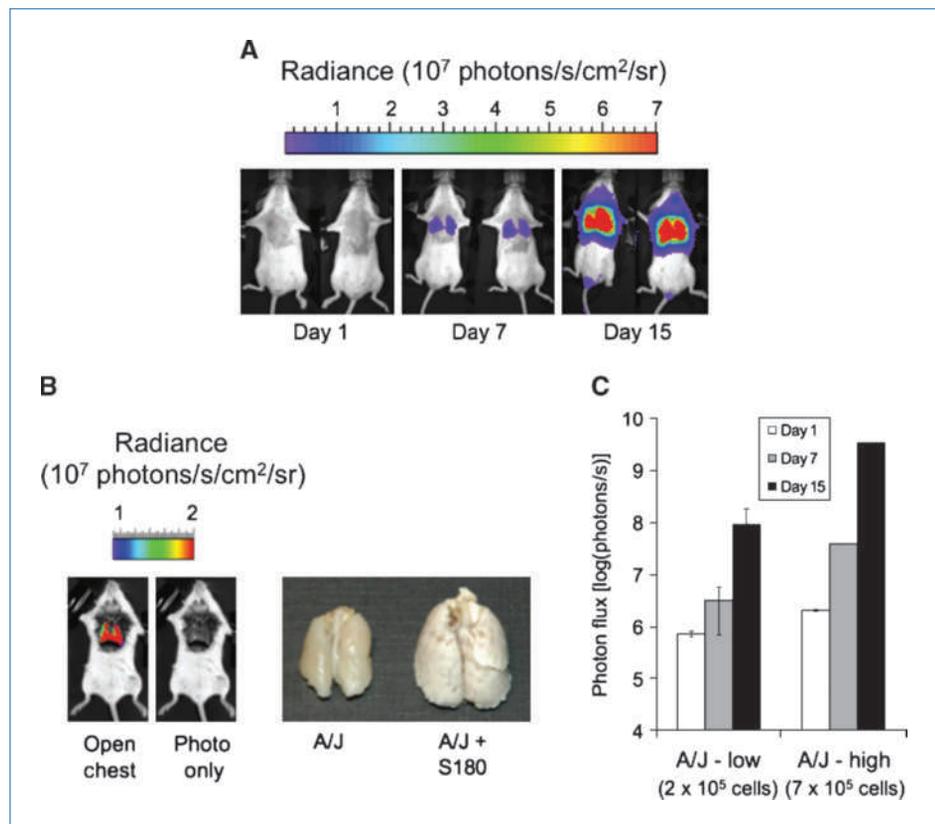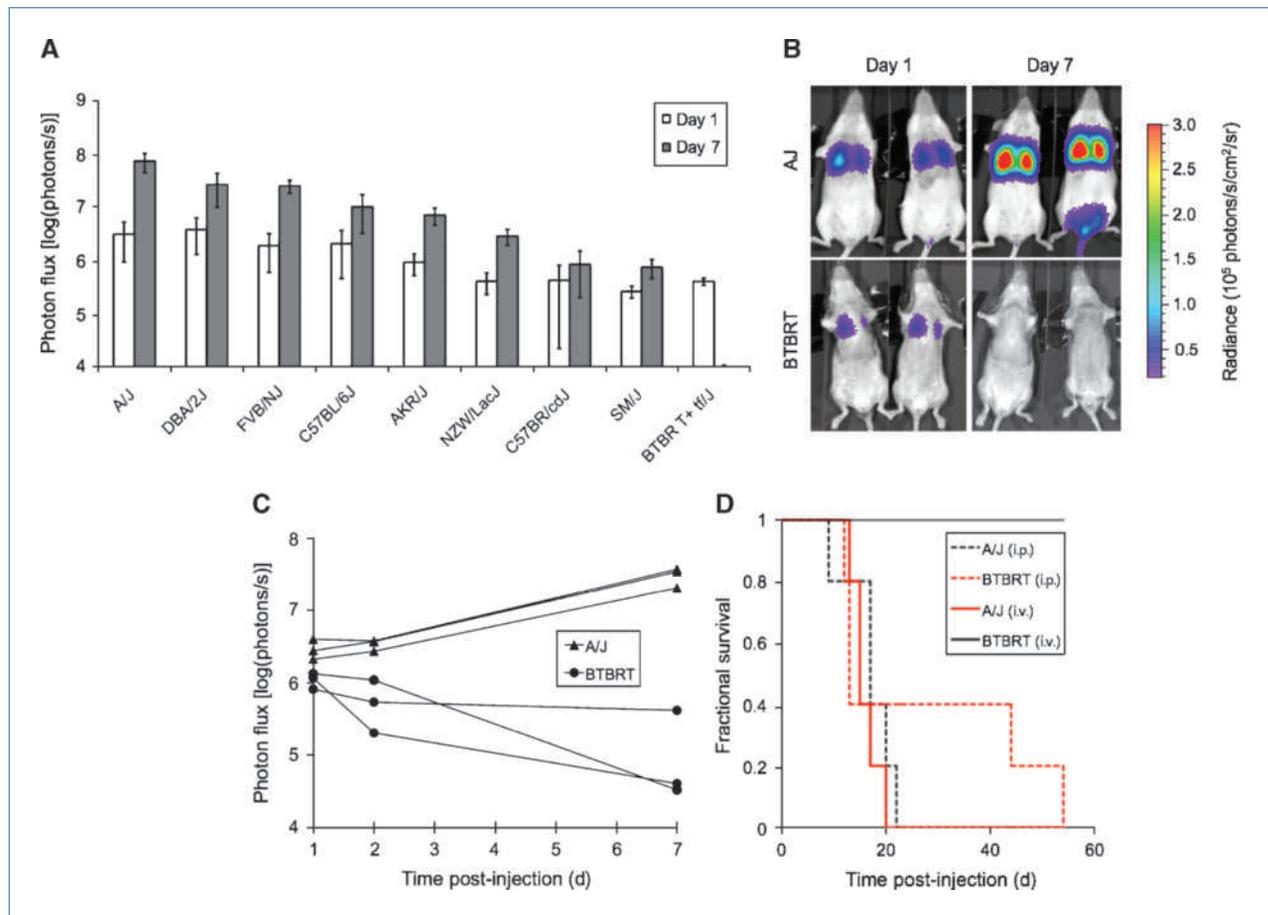
Figure 2. Pulmonary metastasis phenotypes in inbred strains. A, S180-Fluc cells (7×10^5) were tail vein injected in nine strains (see Materials and Methods). Bioluminescence of the lung region was quantified on days 1 and 7 (and background corrected). B, pulmonary metastasis susceptibility in A/J versus BTBRT mice. A/J ($n = 3$) and BTBRT ($n = 3$) mice were tail vein injected with 7×10^5 S180-Fluc cells and bioluminescence was followed in the area over the lungs on days 1, 2, and 7 (shown are two representative mice on days 1 and 7). C, lung bioluminescence was quantified on days 1, 2, and 7 in individual mice of A/J and BTBRT strains. D, survival analysis was done after i.p. and tail vein/i.v. injection of 7×10^5 S180-Fluc cells ($n = 5$ mice per strain).

Histologic assessment of lung tissue after tail vein injection revealed significant differences in tumor cell growth between A/J and BTBRT strains. Lung sections were stained with H&E to evaluate lung architecture, which clearly indicated dense staining of S180-Fluc cell colonization and growth in A/J strain on day 15 (Fig. 3A). The BTBRT strain did not establish any visible tumor nodules, which is consistent with the lack of bioluminescence (Fig. 3A and B). Staining of a representative A/J lung nodule at day 15 with PCNA indicated that these large, proliferative cells are likely the S180 tumor cells (Fig. 3A). Limited proliferative staining was observed in regions with no tumor nodules or in BTBRT mouse lung (Fig. 3B).

To additionally address whether the immune system plays a role in our pulmonary metastasis model, we subjected both A/J and BTBRT strains to supralethal irradiation (18 Gy, cesium-137), which ablates radiosensitive immune cells (20, 21). Approximately 4 hours after irradiation, S180-Fluc cells were tail vein injected and bioluminescence was monitored over 7 days. Irradiated A/J and BTBRT mice were more susceptible to S180-Fluc growth in the lung than nonirradiated controls (Fig. 4). Differences between irradiated and control mice injected were apparent at day 3 for both A/J ($P = 0.0005$) and BTBRT mice ($P = 0.05$). None of the irradiated A/J mice were alive at day 7, presumably due to the rapid growth of tumor cells. At day 7, two of five BTBRT mice were alive and exhibited substantial tumor load compared with control mice, which had completely cleared tumor ($P = 0.0002$). We validated the debilitating effect of supralethal irradiation on the immune system through flow cytometry analysis and observed absence of radiosensitive T-lymphocytes 1 day after irradiation (data not shown).

Previously published data described induction of the innate immune system in response to S180 cell i.p. challenge (15). We therefore assayed a variety of immune cells from whole lung at 1 day after S180-Fluc cell tail vein injection because this was the point at which differences between A/J and BTBRT were observed (Fig. 2C; $P = 0.03$). We examined populations of T cells (CD4+ CD90+ and CD8+ CD90+), natural killer cells (NK1.1+ CD90.2−), macrophages/monocytes

(Cd11b^{lo} CD11c+), dendritic cells (CD11b+ CD11c+), and neutrophils (Ly6G+ GR1+) in A/J and BTBRT strains with and without S180-Fluc challenge. Very few natural killer (NK) cells were found in the lung in the absence or presence of S180 cells, and macrophage, neutrophils, and T-cell populations did not vary significantly with S180 cell challenge (Fig. 5A and B). We observed a significant 2-fold increase in a population of CD11b+ CD11c+ dendritic cells at days 1 and 7, in response to tumor cells in both A/J ($P = 5 \times 10^{-6}$) and BTBRT strains ($P = 0.02$; Fig. 5C and D). Interestingly, we also observed strain-dependent differences in the absolute amount of CD11b+ CD11c+ cells (2-fold, $P = 0.003$), CD4+ T cells (3-fold, $P = 0.00056$), and CD8+ T cells (3-fold, $P = 0.0028$) between A/J and BTBRT strains.

To address the role of T cells in the engraftment and growth of S180 cells in the lungs of BTBRT mice, we injected anti–CD4/CD8 neutralizing antibodies to abrogate T-cell function. We hypothesized that depletion of T cells would enhance pulmonary metastasis. We observed a 40-fold increase in pulmonary engraftment at day 7 (one-tailed t test, $P = 8 \times 10^{-5}$), suggesting that T-cell function is in fact involved in regulating the growth of S180 cells in the lung (Fig. 5E).

Discussion

We have developed an inbred mouse model of pulmonary metastasis using bioluminescence imaging of S180-Fluc cell growth in the lung. Tail vein injection of these cells led to engraftment and growth in the lung at different rates across inbred strains, suggesting a differential host genetic response or susceptibility. This model of "experimental metastasis" suggests a framework for further genetic studies for the identification of genetic variants that underlie the process of pulmonary metastasis. The advantages of this include the ability to measure tumor load across strains using sensitive bioluminescence imaging over a broad dynamic range, short tumor latency, and the consistent targeting and growth in the lung. We also recognize the limitations of our tail vein injection model of S180 cell metastasis to lung. Although this method of delivery of cells is commonly used, and termed experimental metastasis, it bypasses the initial steps of metastasis (i.e., primary site invasion and dissemination). However, it models the later steps of metastasis (i.e., survival, adhesion, extravasation, and colonization). Interestingly, recent evidence suggests that invasion and dissemination can occur early and cells can remain clinically dormant for

Figure 3. Histology of S180-Fluc–injected lungs from A/J and BTBRT strains. AJ and BTBRT mice were tail vein injected with 7×10^5 S180-Fluc cells or media alone. A, lungs were removed on day 15, inflation fixed in Telly's solution, embedded in paraffin, and stained by H&E or anti-PCNA or control antibody as indicated. Representative images were taken at ×100 and ×400 magnifications. B, PCNA staining of A/J and BTBRT lungs. The dotted line indicates an approximate border between the dense, nodular, and highly PCNA-positive stained regions found in A/J mice.
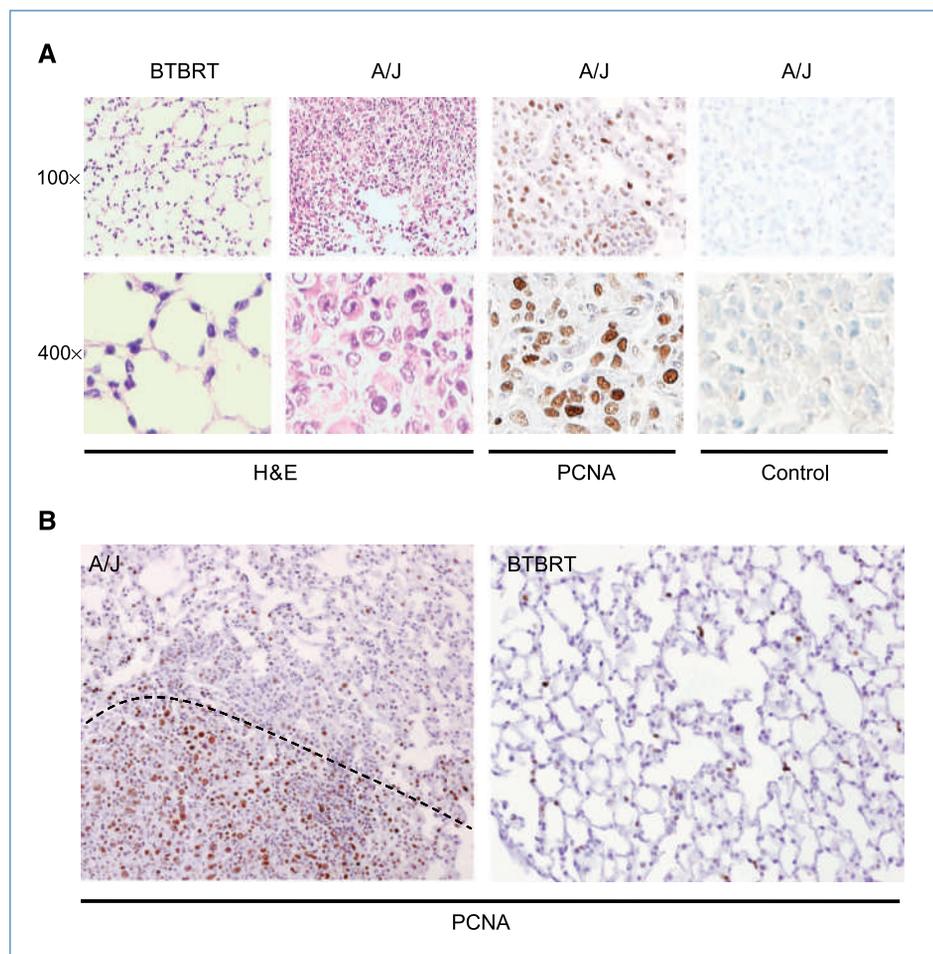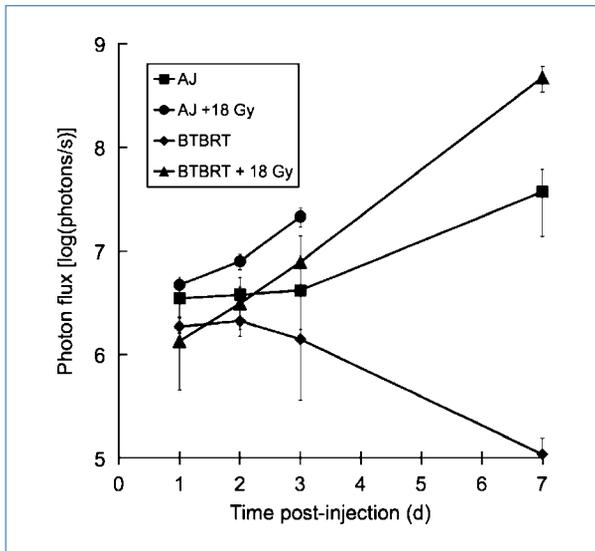
Figure 4. Supralethal irradiation affects pulmonary metastasis susceptibility. A/J and BTBRT mice (n = 5 per group) were irradiated with 18 Gy of cesium-137. Four hours later, they were injected with 7×10^5 S180-Fluc cells and bioluminescent imaging of the lung was done at days 1, 2, 3, and 7. Bars, SD.

extended periods before colonization. These studies have shown that single tumor cells in the bone marrow from breast cancer patients shared few chromosomal aberrations with the breast tumor, suggesting that metastatic cells had left the primary tumor early before clonal expansion in the breast occurred (22, 23). Another recent study showed that normal mammary cells injected via tail vein into the blood stream of a mouse were able to survive in the lungs for up to 16 weeks (24). Subsequent activation of *Myc* and oncogenic *K-Ras* in these cells resulted in tumor growth of the breast cells in the lung. Hence, disseminated normal cells were able to remain "silent" in the lung until receiving signals to promote malignancy.

Genetic control of pulmonary metastasis susceptibility may function through a variety of mechanisms including regulation of adherence, extravasation, angiogenesis, and immune recognition. Clearance of tumor cells may be a function of a differential ability of the immune response to identify and clear tumor cells. As previously mentioned, the unique SR/CR mouse mutant is able to survive repeated i.p. challenges with S180 cells that were otherwise lethal to other inbred strains (14). It was observed that the SR/CR mouse mounted a rapid immunologic response involving NK cells, neutrophils, and macrophages (14, 15). However, the gene(s) and variants responsible for this have yet to be determined. Our observations with the resistant BTBRT strain, which exhibits complete resistance to S180 cells by tail vein injection, may be thought to be analogous to the SR/CR mouse resistance phenotype. However, we observed that BTBRT strain mice are in fact susceptible to death by i.p. introduction of S180 cells, but not by tail vein injection. Hence, the resistance to S180 cells seems to be specific to the envi-

ronment of the lung versus the peritoneal space. Furthermore, we do not observe massive recruitment of neutrophils, macrophages, and NK cells in the lungs of BTBRT mice, which was observed in the peritoneal space of the SR/CR mouse, but rather tumor-dependent changes in dendritic cells and differences in absolute numbers of T cells between strains. This suggests that a different mechanism is responsible for susceptibility phenotypes observed in our model of pulmonary metastasis, and our T-cell depletion experiments show that the cells of the adaptive immune system may very well regulate this process.

Our data using supralethal doses of irradiation suggest that the immune system plays a significant role in the survival and growth of S180-Fluc cells, as tumor growth in both A/J and BTBRT strains was significantly enhanced postirradiation. It has been well established that cells of the immune system, in particular, T lymphocytes, are particularly radiosensitive (20, 21). Although such large radiation doses also cause central nervous system defects and denudation of the gastrointestinal tract, the observation that the BTBRT strain becomes susceptible postirradiation is consistent with an immune-mediated role. These additional consequences of whole-body irradiation are possibly the explanation as to why irradiated and nonirradiated BTBRT mice do not exhibit differences until day 2 to day 3. Whereas tumor vascularization can also be affected by supralethal irradiation, the results of the delayed angiogenesis would most likely result in slower tumor growth, and thus our data further support the assumption that, in our model, irradiation affects immune-mediated clearance of tumor (25–27).

Knowledge of potential mechanisms is important because this can inform future positional cloning efforts after genetic mapping studies. Our studies show that CD11b+ CD11c+ dendritic cell numbers are increased in the lungs of both A/J and BTBRT strains after tumor cell challenge. Although induced in both strains, the higher absolute levels in the BTBRT strain may be responsible for the differential response to tumor. Although dendritic cells typically present antigen to the adaptive immune system, they also possess qualities of innate immune cells because they have been characterized to mediate tumor necrosis factor–mediated apoptotic killing of cancer cells (28, 29). We also observed a larger percentage of both CD8+ (cytotoxic T) and CD4+ (helper T) cells in the lungs of BTBRT mice ($P < 0.05$). Subsequent depletion of these cells through injection of CD4 and CD8 neutralizing antibodies resulted in increased pulmonary engraftment of S180 cells. Hence, T cells clearly play a role in resistance by the BTBRT strain. It is possible that a subset of T cells, T-helper 17 cells, known to highly express IL-17A and which have been shown to be required for inhibition of metastasis of melanoma cells to the lung (30), may be involved in the process. Future experiments will be aimed at elucidating the role of T-helper 17 cells in suppression of metastasis in BTBRT strain.

It remains possible that susceptibility mechanisms include nonimmunologic responses. In human pathologic specimens, tumors that metastasize to the lung are devoid of infiltrating leukocytes (31). In fact, this characteristic is used by pathologists to aid in the determination of whether a malignancy
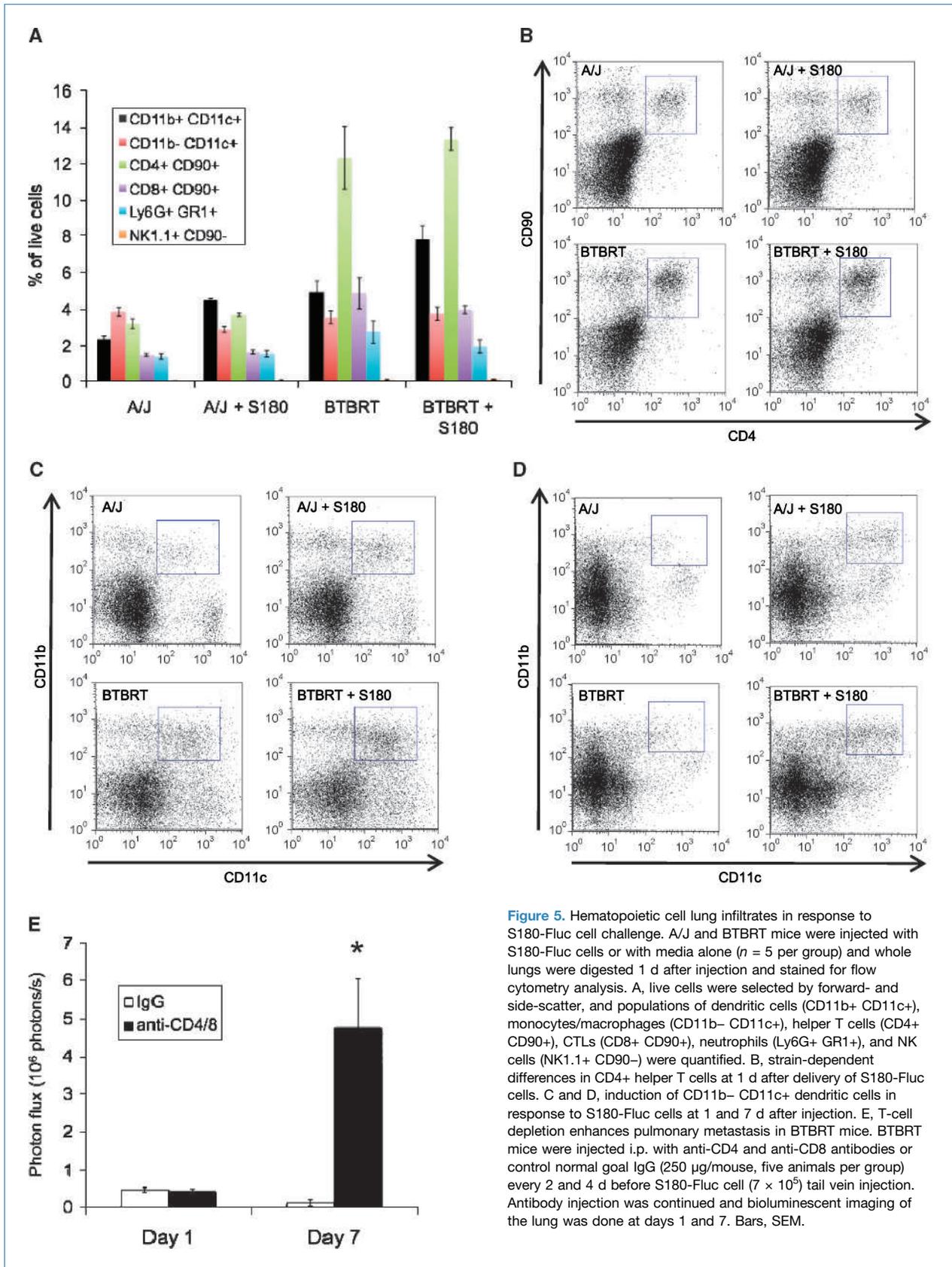
Figure 5. Hematopoietic cell lung infiltrates in response to S180-Fluc cell challenge. A/J and BTBRT mice were injected with S180-Fluc cells or with media alone (n = 5 per group) and whole lungs were digested 1 d after injection and stained for flow cytometry analysis. A, live cells were selected by forward- and side-scatter, and populations of dendritic cells (CD11b+ CD11c+), monocytes/macrophages (CD11b– CD11c+), helper T cells (CD4+ CD90+), CTLs (CD8+ CD90+), neutrophils (Ly6G+ GR1+), and NK cells (NK1.1+ CD90–) were quantified. B, strain-dependent differences in CD4+ helper T cells at 1 d after delivery of S180-Fluc cells. C and D, induction of CD11b– CD11c+ dendritic cells in response to S180-Fluc cells at 1 and 7 d after injection. E, T-cell depletion enhances pulmonary metastasis in BTBRT mice. BTBRT mice were injected i.p. with anti-CD4 and anti-CD8 antibodies or control normal goal IgG (250 μg/mouse, five animals per group) every 2 and 4 d before S180-Fluc cell (7×10^5) tail vein injection. Antibody injection was continued and bioluminescent imaging of the lung was done at days 1 and 7. Bars, SEM.

located in the human lung is a primary or metastatic tumor. It is thus probable that "edited" metastatic tumors are unrecognized by the immune system, raising the possibility that host genetics determining the growth pattern of such tumors are nonimmunologic in nature (e.g., growth, angiogenic, and tropic factors) and shaped mostly by local "tissue intrinsic" factors present at the specific site of metastasis. We tested to see if there was any increased detection of apoptosis in A/J and BTBRT lungs at 1 and 7 days after S180 injection; however, no tumor- or strain-dependent changes were observed (data not shown). Nevertheless, we remain open to the possibility that tissue intrinsic factors shape the susceptibility to metastasis. It is also possible that day 1 and day 7 phenotypes may describe different processes. The day 1 phenotype could model the ability for the tumor to seed in the lung, and the day 7 phenotype could model the ability to survive, extravasate, colonize, and grow in the lung.

It is important to note that metastasis of a primary cancer can occur much earlier than the initial clinical diagnosis of the primary cancer. Some patients can present with metastatic disease and have an unknown primary disease or well-differentiated tumor, suggesting that dissemination of tumor cells can occur early. Hence, discovery of genetic susceptibility variants and then development of preventive protocols in model organisms, such as inbred mice, would aid in the understanding and treatment of the human condition.

Our study forms the basis of an inbred mouse model of cancer cell metastasis to the lung that shows differential metastatic load in a variety of inbred strains. These observations also suggest that gene loci responsible for S180 cell growth have the potential to be mapped through A/J ×

BTBRT F2 linkage mapping. In addition, recent advances in single-nucleotide polymorphism discovery have provided researchers with the necessary resources to explore a wide range of genetic variation in laboratory mice (32). The use of dense SNP maps in inbred mice has proved successful in the identification and fine mapping of major quantitative trait loci and the identification of new genetic determinants of complex traits (33–37). Hence, the measurement of S180-induced pulmonary metastasis in 30+ inbred mouse strains would permit the use of genome-wide association studies to enhance susceptibility gene discovery and is a current focus of our laboratory.

Disclosure of Potential Conflicts of Interest

Acknowledgments

Grant Support

References

1. Wittekind C, Neid M. Cancer invasion and metastasis. Oncology 2005;69 Suppl 1:14–6.
2. Joyce JA, Pollard JW. Microenvironmental regulation of metastasis. Nat Rev Cancer 2009;9:239–52.
3. Weiss L. Metastatic inefficiency. Adv Cancer Res 1990;54:159–211.
4. The organ preference of metastasis formation. Molecular mechanisms of cancer. pp. 361–82007.
5. Songur N, Dinc M, Ozdilekcan C, Eke S, Ok U, Oz M. Analysis of lung metastases in patients with primary extremity sarcoma. Sarcoma 2003;7:63–7.
6. Mehlen P, Puisieux A. Metastasis: a question of life or death. Nat Rev Cancer 2006;6:449–58.
7. Nguyen DX, Massague J. Genetic determinants of cancer metastasis. Nat Rev Genet 2007;8:341–52.
8. Khanna C, Hunter K. Modeling metastasis *in vivo*. Carcinogenesis 2005;26:513–23.
9. Greenberg NM, DeMayo F, Finegold MJ, et al. Prostate cancer in a transgenic mouse. Proc Natl Acad Sci U S A 1995;92:3439–43.
10. Lifsted T, Le Voyer T, Williams M, et al. Identification of inbred mouse strains harboring genetic modifiers of mammary tumor age of onset and metastatic progression. Int J Cancer 1998;77:640–4.
11. Alfaro G, Lomeli C, Ocadiz R, et al. Immunologic and genetic characterization of S180, a cell line of murine origin capable of growing in different inbred strains of mice. Vet Immunol Immunopathol 1992;30:385–98.
12. Tarnowski GS, Mountain IM, Stock CC. Influence of genotype of host on regression of solid and ascitic forms of sarcoma 180 and effect of chemotherapy on the solid form. Cancer Res 1973;33:1885–8.
13. Cui Z, Willingham MC, Hicks AM, et al. Spontaneous regression of advanced cancer: identification of a unique genetically determined, age-dependent trait in mice. Proc Natl Acad Sci U S A 2003;100:6682–7.
14. Hicks AM, Riedlinger G, Willingham MC, et al. Transferable anticancer innate immunity in spontaneous regression/complete resistance mice. Proc Natl Acad Sci U S A 2006;103:7753–8.
15. Hicks AM, Willingham MC, Du W, Pang CS, Old LJ, Cui Z. Effector mechanisms of the anti-cancer immune responses of macrophages in SR/CR mice. Cancer Immun 2006;6:11.
16. Kesarwala AH, Prior JL, Sun J, Harpstrite SE, Sharma V, Piwnica-Worms D. Second-generation triple reporter for bioluminescence, micro-positron emission tomography, and fluorescence imaging. Mol Imaging 2006;5:465–74.
17. Gross S, Piwnica-Worms D. Real-time imaging of ligand-induced IKK activation in intact cells and in living mice. Nat Methods 2005;2:607–14.
18. Gross S, Piwnica-Worms D. Monitoring proteasome activity in cellulo and in living animals by bioluminescent imaging: technical considerations for design and use of genetically encoded reporters. Methods Enzymol 2005;399:512–30.
19. Okazaki M, Krupnick AS, Kornfeld CG, et al. A mouse model of orthotopic vascularized aerated lung transplantation. Am J Transplant 2007;7:1672–9.
20. Kajioka EH, Andres ML, Li J, et al. Acute effects of whole-body proton irradiation on the immune system of the mouse. Radiat Res 2000;153:587–94.
21. Van der Meeren A, Mouthon MA, Gaugler MH, Vandamme M,

Gourmelon P. Administration of recombinant human IL11 after su-pralethal radiation exposure promotes survival in mice: interactive effect with thrombopoietin. Radiat Res 2002;157:642–9.

22. Schardt JA, Meyer M, Hartmann CH, et al. Genomic analysis of single cytokeratin-positive cells from bone marrow reveals early mutational events in breast cancer. Cancer Cell 2005;8:227–39.

23. Schmidt-Kittler O, Ragg T, Daskalakis A, et al. From latent disseminated cells to overt metastasis: genetic analysis of systemic breast cancer progression. Proc Natl Acad Sci U S A 2003;100:7737–42.

24. Podsypanina K, Du YC, Jechlinger M, Beverly LJ, Hambardzumyan D, Varmus H. Seeding and propagation of untransformed mouse mammary cells in the lung. Science 2008;321:1841–4.

25. Hopewell J, Withers HR. Proposition: long-term changes in irradiated tissues are due principally to vascular damage in the tissues. Med Phys 1998;25:2265–8.

26. Murray C. Inflammatory cytokines, radiation, and endothelial gene products: a common role for reactive oxygen intermediates. In: Rubin DB, editor. The radiation biology of the vascular endothelium. Berlin: Springer; 1998, p. 147–56.

27. Paris F, Fuks Z, Kang A, et al. Endothelial apoptosis as the primary lesion initiating intestinal radiation damage in mice. Science 2001;293:293–7.

28. Janjic BM, Lu G, Pimenov A, Whiteside TL, Storkus WJ, Vujanovic NL. Innate direct anticancer effector function of human immature dendritic cells. I. Involvement of an apoptosis-inducing pathway. J Immunol 2002;168:1823–30.

29. Lu G, Janjic BM, Janjic J, Whiteside TL, Storkus WJ, Vujanovic NL. Innate direct anticancer effector function of human immature dendritic cells. II. Role of TNF, lymphotoxin-$\alpha_1\beta_2$, Fas ligand, and TNF-related apoptosis-inducing ligand. J Immunol 2002;168:1831–9.

30. Martin-Orozco N, Muranski P, Chung Y, et al. T helper 17 cells promote cytotoxic T-cell activation in tumor immunity. Immunity 2009; 31:787–98.

31. Ioachim HL. Immunobiology of metastases. Cancer Detect Prev 1991;15:127–31.

32. Wade CM, Daly MJ. Genetic variation in laboratory mice. Nat Genet 2005;37:1175–80.

33. Liu PY, Lu Y, Deng HW. Accurate haplotype inference for multiple linked single-nucleotide polymorphisms using sibship data. Genetics 2006;174:499–509.

34. Grupe A, Germer S, Usuka J, et al. In silico mapping of complex disease-related traits in mice. Science 2001;292:1915–8.

35. Liao G, Wang J, Guo J, et al. In silico genetics: identification of a functional element regulating H2-Eα gene expression. Science 2004;306:690–5.

36. Pletcher MT, McClurg P, Batalov S, et al. Use of a dense single nucleotide polymorphism map for in silico mapping in the mouse. PLoS Biol 2004;2:e393.

37. Valdar W, Solberg LC, Gauguier D, et al. Genome-wide genetic association of complex traits in heterogeneous stock mice. Nat Genet 2006;38:879–87.

Cancer Research

The Journal of Cancer Research (1916–1930) | The American Journal of Cancer (1931–1940)

Strain-Specific Susceptibility for Pulmonary Metastasis of Sarcoma 180 Cells in Inbred Mice

Haris G. Vikis, Erin N. Jackson, Alexander S. Krupnick, et al.

Updated version	Access the most recent version of this article at: doi:10.1158/0008-5472.CAN-09-4177

Cited articles	This article cites 35 articles, 11 of which you can access for free at: http://cancerres.aacrjournals.org/content/70/12/4859.full#ref-list-1

E-mail alerts	Sign up to receive free email-alerts related to this article or journal.
Reprints and Subscriptions	To order reprints of this article or to subscribe to the journal, contact the AACR Publications Department at pubs@aacr.org.
Permissions	To request permission to re-use all or part of this article, use this link http://cancerres.aacrjournals.org/content/70/12/4859. Click on "Request Permissions" which will take you to the Copyright Clearance Center's (CCC) Rightslink site.